Heliyon 10 (2024) e32886

Contents lists available at ScienceDirect

Heliyon

journal homepage: www.cell.com/heliyon

Research article

SNF1 plays a crucial role in the utilization of *n*-alkane and transcriptional regulation of the genes involved in it in the yeast *Yarrowia lipolytica*

Napapol Poopanitpan [a,b], Sorawit Piampratom [b], Patthanant Viriyathanit [a], Threesara Lertvatasilp [a], Hiroyuki Horiuchi [c,d], Ryouichi Fukuda [c,d], Pichamon Kiatwuthinon [a,*]

[a] *Department of Biochemistry, Faculty of Science, Kasetsart University, Chatuchak, Bangkok, 10900, Thailand*
[b] *Interdisciplinary Program in Genetic Engineering, The Graduate School, Kasetsart University, Chatuchak, Bangkok, 10900, Thailand*
[c] *Department of Biotechnology, The University of Tokyo, Yayoi 1-1-1, Bunkyo-ku, Tokyo, 113-8657, Japan*
[d] *Collaborative Research Institute for Innovative Microbiology, The University of Tokyo, Yayoi 1-1-1, Bunkyo-ku, Tokyo, 113-8657, Japan*

ARTICLE INFO

Keywords:
Yarrowia lipolytica
YlSNF1
n-alkane utilization
Lipid metabolism
Transcriptomics analysis

ABSTRACT

Yarrowia lipolytica is an ascomycetous yeast that can assimilate hydrophobic carbon sources including oil and *n*-alkane. The sucrose non-fermenting 1/AMP-activated protein kinase (Snf1/AMPK) complex is involved in the assimilation of non-fermentable carbon sources in various yeasts. However, the role of the Snf1/AMPK complex in *n*-alkane assimilation in *Y. lipolytica* has not yet been elucidated. This study aimed to clarify the role of *Y. lipolytica SNF1* (*YlSNF1*) in the utilization of *n*-alkane. The deletion mutant of *YlSNF1* (Δ*Ylsnf1*) exhibited substantial growth defects on *n*-alkanes of various lengths (C10, C12, C14, and C16), and its growth was restored through the introduction of *YlSNF1*. Microscopic observations revealed that *Yl*Snf1 tagged with enhanced green fluorescence protein showed dot-like distribution patterns in some cells cultured in the medium containing *n*-decane, which were not observed in cells cultured in the medium containing glucose or glycerol. The RNA sequencing analysis of Δ*Ylsnf1* cultured in the medium containing *n*-decane exhibited 302 downregulated and 131 upregulated genes compared with the wild-type strain cultured in the same medium. Gene ontology and Kyoto Encyclopedia of Genes and Genomes enrichment analyses suggested that a significant fraction of the downregulated genes functioned in peroxisomes or were involved in the metabolism of *n*-alkane and fatty acids. Quantitative real-time PCR analysis confirmed the downregulation of 12 genes involved in the metabolism of *n*-alkane and fatty acid, *ALK1–ALK3*, *ALK5*, *ADH7*, *PAT1*, *POT1*, *POX2*, *PEX3*, *PEX11*, *YAS1*, and *HFD3*. Furthermore, Δ*Ylsnf1* exhibited growth defects on the medium containing the metabolites of *n*-alkane (fatty alcohol and fatty aldehyde). These findings suggest that *YlSNF1* plays a crucial role in the utilization of *n*-alkane in *Y. lipolytica*. This study provides important insights into the advanced biotechnological applications of this yeast, including the bioconversion of *n*-alkane to useful chemicals and the bioremediation of petroleum-contaminated environments.

* Corresponding author. Department of Biochemistry, Faculty of Science, Kasetsart University, 50 Ngamwongwan Rd., Ladyao, Chatuchak, 10900, Bangkok, Thailand.
E-mail address: fscipmk@ku.ac.th (P. Kiatwuthinon).

https://doi.org/10.1016/j.heliyon.2024.e32886
Received 24 January 2024; Received in revised form 10 June 2024; Accepted 11 June 2024
Available online 12 June 2024

1. Introduction

Yarrowia lipolytica, classified as an ascomycetous yeast [1], can utilize non-fermentable carbon sources, including glycerol, alcohols, and hydrophobic substrates such as fat, fatty acids, and *n*-alkanes, as its sole carbon and energy sources [2,3]. This superior feature allows *Y. lipolytica* to be employed as a sustainable tool for a wide range of applications, particularly in the bioconversion of *n*-alkane to useful chemicals and bioremediation of *n*-alkane-contaminated environments [4,5]. Therefore, a comprehensive understanding of the metabolic pathway of *n*-alkane in *Y. lipolytica* and its control mechanisms could further promote the advanced utilization of this yeast.

The metabolic pathways of *n*-alkane and the enzymes involved in it in *Y. lipolytica* have been clarified [3,6]. In the assimilation of *n*-alkane, several oxidative enzymes in the endoplasmic reticulum (ER) and peroxisomes are involved [6–9]. Cytochrome P450ALK, a member of the CYP52 family, plays a primary role in the initial hydroxylation of *n*-alkanes to fatty alcohols on the ER membrane [10,11]. *Y. lipolytica* contains 12 genes (*ALK1-ALK12*) that encode proteins homologous to the P450 of the CYP52 family. Among the Alk proteins, Alk1 and Alk2 play a vital role in the assimilation of *n*-alkane in *Y. lipolytica* [10,11]. In addition, while Alk9 and Alk10 have *n*-alkane-hydroxylating activities, Alk3 and Alk6 have significant activities to hydroxylate both *n*-alkanes and dodecanoic acid [10,11]. Further oxidation of fatty alcohols to fatty aldehydes is mediated by fatty alcohol dehydrogenases (FADH) in the ER and fatty alcohol oxidase (FAO) in peroxisomes [7,12,13]. *Y. lipolytica* contains eight alcohol dehydrogenase genes (*ADH1-ADH7* and *FADH)* and one FAO gene (*FAO1)*. Among these genes, *ADH1*, *ADH3*, and *FAO1* are involved in the oxidation of exogenous fatty alcohol [7,12,13]. Fatty aldehydes are then oxidized to fatty acids by fatty aldehyde dehydrogenases (FALDHs) in the ER or peroxisome [7,12,13]. *Y. lipolytica* has four FALDH genes, *HFD1-HFD4*, which are involved in the oxidation of fatty aldehydes produced during the metabolism of *n*-alkanes [7,12,13]. The fatty acids are activated to acyl-CoAs by acyl-CoA synthetases (ACS) to be metabolized via β-oxidation in the peroxisome or for the synthesis of various lipids [3,7,14]. *Y. lipolytica* contains 15 genes, *FAA1*, *FAT1* – *FAT4*, and *AAL1* – *AAL10*, which encode ACSs. *FAT1* is involved in the activation of fatty acids produced during the metabolism of *n*-alkane in the peroxisome for assimilation, whereas *FAA1* participates in the activation of fatty acids for lipid synthesis [14]. *AAL4* and *AAL7* are involved in the activation of exogenous fatty acids in peroxisome [15].

The metabolism of *n*-alkane in *Y. lipolytica* is regulated at transcriptional levels [6,16,17]. The expression of *ALK1* is upregulated in response to *n*-alkane by a heterocomplex composed of the basic helix-loop-helix (bHLH) transcription factors Yas1 and Yas2 and is downregulated by the Opi1-family transcription repressor Yas3 [16,18]. Yas1 and Yas2 constitutively localize in the nucleus and bind to alkane-responsive element 1 (ARE1) on the *ALK1* promotor [16,18]. In the absence of *n*-alkanes, Yas3 enters the nucleus where it binds to Yas2 and represses *ALK1* transcription. In the presence of *n*-alkanes, Yas3 is retained in the ER membrane, and the transcription of *ALK1* is activated by the Yas1 and Yas2 complex. The molecular mechanism by which Yas3 is retained in the ER is unclear; however, Yas3 can bind to phosphatidic acid and phosphoinositides *in vitro*, raising the possibility that Yas3 is retained in the ER by binding to these phospholipids [16]. In addition to the Yas1-Yas2-Yas3 system, Por1, which is a homolog of FarA of *Aspergillus nidulans*, was demonstrated to be involved in the transcriptional regulation of β-oxidation genes and peroxisome-related genes, including *POT1*, *PAT1*, *POX2*, and *PEX5*, in response to fatty acid [19].

Another regulatory system associated with non-fermentable carbon source metabolism in yeast involves sucrose non-fermenting 1 (Snf1) protein kinase, a homolog of mammalian AMP-activated protein kinase (AMPK) [20]. In *Saccharomyces cerevisiae*, one of the most intensively studied yeasts, *Sc*Snf1 forms a heterotrimeric complex as an α catalytic subunit with a γ regulatory subunit (Snf4) and one of the three β subunits (Sip1, Sip2, or Gal83) [20]. *Sc*Snf1 exerts regulatory functions at the transcriptional and post-translational levels [20]. It has been reported to play crucial roles in a wide range of cellular processes, including aging, meiosis, autophagy, glycogen accumulation, and stress responses, depending on its localization with its β subunits in the cells [20–23]. Snf1 is involved in the growth on several alternative carbon sources, such as glycerol and ethanol, via glucose derepression [22]. In a glucose-rich medium, the *Sc*Snf1 interacts with its three β subunits and is distributed throughout the cytoplasm, excluding the nucleus. When cultured in media containing nonfermentable carbon sources, some Snf1 complexes relocate to various organelles for specific functions. Snf1-Gal83 and Snf1-Sip1 specifically relocate from the cytoplasm to the nucleus and vacuole, respectively, whereas Snf1-Sip2 remains in the cytoplasm [23–25]. In *Y. lipolytica*, Snf1 (*Yl*Snf1) has been reported to function as a negative regulator of lipid accumulation [26]. The deletion mutant of *YlSNF1* strain cultured in a glucose-containing medium exhibited a dramatic increase in lipid accumulation and upregulation of the transcription of genes involved in lipid metabolism. However, the role of *Yl*Snf1 in the utilization of an *n*-alkane and its regulation remains unclear. Hence, this study aims to clarify the roles of *Yl*Snf1 through an analysis of the growth on *n*-alkane and its metabolites, the subcellular localization of *Yl*Snf1, and the alternation in the global gene expression profiles of Δ*Ylsnf1* cultured in the medium containing *n*-alkane. Our results suggest that *Yl*Snf1 plays a crucial role in the utilization of *n*-alkane in *Y. lipolytica*. The findings of this study provide important insights into the metabolism of *n*-alkane and its regulation in *Y. lipolytica*.

2. Material and methods

2.1. Yeast strains, media, and growth condition

Y. lipolytica strain CXAU/A1 (*ura3*, *ade1*:*ADE1*) [27] was used as the wild-type strain. YNB medium (0.17 % (w/v) yeast nitrogen base without amino acids and ammonium sulfate; Difco, 0.5 % (w/v) ammonium sulfate) was used as the liquid medium and supplemented with different carbon sources as follows: 2 % (w/v) glycerol, 2 % (w/v) glucose, or 2 % (v/v) *n*-decane. For the solid media, the YNB medium was mixed with 0.1 % fatty acids (lauric acid, myristic acid, palmitic acid, or oleic acid), 1-dodecanol, and dodecanal,

Table 1
Sequences and purposes of primers used in this study.

Primer name	Sequences	Purpose	Primer references
YALI0D02101-5F	GCTCTAGAGGGTGAAGCGGGAAATCAAG	Deletion cassette	This study
YALI0D02101-5R	CGGGATCCTTGTGAGGTGGTGGAAGGAG	Deletion cassette	This study
YALI0D02101-3F	CGGGATCCGCACTTGTAGAGCACACTAG	Deletion cassette	This study
YALI0D02101-3R	CCGCTCGAGCGAATTGCACCAGTCGTTC	Deletion cassette	This study
YalD02101SH-5F	CCCGTCGACAAGCTTGGGTGAAGCGGGAAATCAAG	pSNF1	This study
YalD02101H-3R	CCCAAGCTTCGAATTGCACCAGTCGTTCA	pSNF1	This study
101-fusion-R	AATCCCTAGTGTGCTCTACAAGTGCTTAGGCGCCCCTAGGCTTCTCACTCTCCTTCTGAGAACTCAC	pSNF1-EGFP	This study
101-fusion-F	GTGAGTTCTCAGAAGGAGAGTGAGAAGCCTAGGGGCGCCTAAGCACTTGTAGAGCACACTAGGGAT	pSNF1-EGFP	This study
EGFP-*Avr*II-F	GGCCTAGGATGGTGAGCAAGGGCGAGGA	pSNF1-EGFP	This study
EGFP-Kas-R	GGGGCGCCCTTGTACAGCTCGTCCATGCC	pSNF1-EGFP	This study
ALK1-F	AGTGGAAGTGTGGTAAGCCCAA	Realtime RT-PCR	[39]
ALK1-R	CAAACTCGAGCAGTCGGTTCTT	Realtime RT-PCR	[39]
ALK2-F	ACTTGGCCTTTTCCGATCCTT	Realtime RT-PCR	[39]
ALK2-R	TTGAACTGAGTGGCCAGAACG	Realtime RT-PCR	[39]
ALK3-F	CGCTCGAAAAGAAAAGTCCGA	Realtime RT-PCR	[39]
ALK3-R	GGTCCCGCAAAGTGATCTTGT	Realtime RT-PCR	[39]
ALK5-F	TTTCATTCCCAAAGGCCAGAC	Realtime RT-PCR	[39]
ALK5-R	CCCATCGCTCAGGAATGAACT	Realtime RT-PCR	[39]
PAT1qF	TTACCAAGGACGACATTGCCCT	Realtime RT-PCR	This study
PAT1qR	CCTTGACGTTGACCTTGGACTT	Realtime RT-PCR	This study
POT1qF	TCGAGTCCATGTCCAACCAGT	Realtime RT-PCR	This study
POT1qR	GGCAACGTTCTCGGAAGTGAT	Realtime RT-PCR	This study
POX2qF	TCTCAACAAGGAGCAGATCCGAG	Realtime RT-PCR	This study
POX2qR	ATCGCTTCTTGATGTCGTCCTCG	Realtime RT-PCR	This study
PEX11-F	AGTTCTCCATGGCCCGAAAG	Realtime RT-PCR	This study
PEX11-R	GGCCAATGGTTGTGTATCGC	Realtime RT-PCR	This study
PEX3-F	GCGTGCTAAGGAGAGACTCA	Realtime RT-PCR	This study
PEX3-R	TCGACAGCCACAAACTCCAT	Realtime RT-PCR	This study
YAS1-F	GGGTTTGAGCGCATCACCAA	Realtime RT-PCR	This study
YAS1-R	GGTTCTTCAAAAAGGCCACCG	Realtime RT-PCR	This study
ADH7-F	CGAGGAAGTCAACGGACCTT	Realtime RT-PCR	This study
ADH7-R	GTGGCAGACACCGGAATACT	Realtime RT-PCR	This study
HFD3-F	CAGGTTGATTACGTCACAAGAAAC	Realtime RT-PCR	[13]
HFD3-R	AATGACCTCGTTGATGTTTACAGA	Realtime RT-PCR	[13]
H3X-AK-F	CTAGGTACCCCTACGACGTCCCCGACTACGCCTATCCTTATGATGTTCCCGACTATGCTTATCCCTACGACGTGCCTGATTATGCTG	pSNF1-HA	This study
H3X-AK-R	GCGCCAGCATAATCAGGCACGTCGTAGGGATAAGCATAGTCGGGAACATCATAAGGATAGGCGTAGTCGGGGACGTCGTAGGGGTAC	pSNF1-HA	This study

and dispersed in 0.05 % (v/v) Triton X-100. In addition, *n*-alkanes (*n*-decane, *n*-dodecane, *n*-tetradecane, and *n*-hexadecane) were supplied to the YNB solid medium in the vapor phase. Uracil (24 mg/L) was added when necessary. All the yeast strains were grown at 30 °C.

The deletion mutant of *YlSNF1* was generated from CXAU1 using a deletion cassette constructed by amplifying upstream and downstream flanking coding regions of *YlSNF1* (*Yal0ID02101g*) from the genomic DNA of CXAU1 using the YALI0D02101-5F/YALI0D02101-5R and YALI0D02101-3F/YALI0D02101-3R primers, respectively (Table 1). The amplified upstream and downstream fragments were double-digested with *Bam*HI-*Xba*I and *Bam*HI-*Xho*I, respectively. Then, the fragments were cloned into the *Xba*I-*Xho*I site of pBluescript II SK(+) to obtain pUDSNF1. An *ADE1* fragment was obtained from pSAT4 by digestion with *Bam*HI and inserted into the *Bam*H1 site of pUDSNF1, generating the pDELSNF1 plasmid. Subsequently, the pDELSNF1 plasmid was used as a template to amplify the deletion cassette using the YALI0D02101-5F and YALI0D02101-3R primers, as shown in Table 1. The amplified cassette was introduced into CXAU1 cells to generate the Δ*Ylsnf1* strain. For growth analysis, all strains were cultured for 2 days in SG medium, and spotted on the agar plates containing indicated carbon sources in 10-fold serial dilutions starting with 5 μL of 1 OD_{600} units/mL. Then, the strains were incubated at 30 °C for 2-3 days on glycerol and glucose and 4 days on oleic acid, palmitic acid myristic acid, lauric acid, *n*-decane, *n*-dodecane, *n*-tetradecane, and *n*-hexadecane.

2.2. Plasmid construction

The plasmid pSNF1, to express *YlSNF1* under its native promoter in *Y. lipolytica*, was constructed as follows. The *YlSNF1* gene containing its upstream and downstream flanking coding regions was amplified from the genomic DNA of CXAU1 by PCR using the YalD02101SH-5F and YalD02101H-3R primers shown in Table 1. Next, the amplified *YlSNF1* was digested with *Hin*dIII and cloned into the *Hin*dIII site of pSUT5 [28]. Plasmid pSNF1-EGFP, which expresses *Yl*Snf1 fused with an enhanced green fluorescent protein (EGFP) at its C-terminus under the control of *YlSNF1* native promoter, was constructed as follows. The ORF of the *YlSNF1* gene, with its upstream and downstream flanking regions, was amplified from the genomic DNA of CXAU1 using PCR with primers YalD02101SH-5F and 101-fusion-R, and 101-fusion-F and YalD02101H-3R, respectively (Table 1). These two amplified fragments were cut and cloned into the *Hin*dIII site of pSUT5-nonAvrII to obtain plasmid p101-GT. Next, the ORF of EGFP was amplified by PCR using EGFP-*Avr*II-F and EGFP-Kas-R and cloned into the *Avr*II-*Kas*I sites of p101-GT to obtain pSNF1-EGFP. An oligonucleotide fragment of 3X human influenza hemagglutinin (HA) was inserted into the *Avr*II-*Kas*I sites of p101-GT to obtain pSNF1-HA.

2.3. Transformation

Y. lipolytica was transformed by electroporation as described previously in Ref. [29].

2.4. RNA extraction and RNA sequencing (RNA-seq)

Two strains, CXAU/A1 and *ΔYlsnf1*, were pre-cultured in uracil-containing SG medium for 48 h at 30 °C. Next, the cell densities were adjusted to an optical density of 0.05, and cultured in a uracil-containing SG medium for 24 h at 30 °C. Subsequently, the cells were washed with the YNB medium twice and cultured in YNB medium with uracil containing 2 % *n*-decane for 1 h at 30 °C. Next, 0.1 % (v/v) triton-X 100 was added to separate the cells from *n*-decane droplets in the medium. The cells were collected and used for RNA extraction. Briefly, ISOGEN (Nippon Gene, Japan) was added, and the cells were lysed using a glass bead shocker, followed by chloroform extraction. The genomic DNA was removed from the samples by treating them with an RNase-free DNase I (Omega Biotek; Norcross, GA, USA). The quality and concentration of the extracted RNA were determined using a Nanodrop photometer (Thermo Scientific, Waltham, MA, USA). RNA samples with A260/280 and A260/230 higher than 2.0 were used for RNA sequencing or cDNA synthesis.

2.5. RNA-seq and data analysis

The RNA library was prepared using a TruSeq Strand mRNA Library Preparation Kit (Illumina, San Diego, CA, USA). All libraries were sequenced using the Illumina Nova Seq 6000 (Illumina, San Diego, CA, USA) with 2 × 150 bp paired-end sequencing flow cells, according to the manufacturer's protocol. The FASTQ data were deposited in the GEO database (GSE 215766). The FASTQ files obtained from RNA-seq were analyzed using tools on the Galaxy platform (https://usegalaxy.org/) with default parameters. First, the sequence reads were trimmed for adapter sequences using Trimmomatic (Galaxy Version 0.38.0), followed by alignment of the sequence reads against the reference genome assembly ASM252v1 using the HISAT2 program (Galaxy Version 2.2.1+ galaxy0). Mapped sequences were assembled and quantified using StringTie and StringTie Merge (Galaxy Version 2.1.7+ galaxy1). The differentially expressed counts between the wild-type and mutant-assembled transcripts were estimated using DESeq2 (Galaxy Version 2.11.40.7+ galaxy1). Differentially expressed genes (DEGs) were annotated using Annotate DESeq2/DEXSeq output tables (Galaxy Version 1.1.0), and the expression data were shown as $\log_2$(fold change) ($\log_2$FC). The false discovery rate was controlled with a *P*-value <0.05. The DEGs with $\text{Log}_2\text{FC} \geq 2.5$ and adj P-value <0.05 were submitted to DAVID (https://david.ncifcrf.gov/), a free web server to perform the functional enrichment analysis and gene ontology (GO) analysis.

2.6. cDNA synthesis and quantitative real time PCR (qRT-PCR)

A sample (2 μg) of extracted RNA was reverse transcribed into cDNA using a RevertAid cDNA Synthesis Kit (Thermo Fisher Scientific; Waltham, MA, USA) according to the manufacturer's protocol. Next, qRT-PCR was performed to validate the RNA-seq result and to determine the relative gene expression of the specific genes using the primers indicated in Table 1, with iTaq™ Universal SYBR® Green Supermix (Bio-Rad, Hercules, CA, USA) in a CFX Connect™ Real-Time System (Bio-Rad, Hercules, CA, USA). The thermocycling protocol was as follows: denaturation at 95 °C for 3 min, extension at 95 °C for 30 s, 59.5 °C for 30 s, and 72 °C for 45 s (40 cycles), and a final extension at 72 °C for 10 min. The β-actin gene was used an internal control for normalization of gene expression. The quantification cycle (Cq) values were used to calculate the relative gene expression using the ΔΔCq method.

2.7. Fluorescence microscopy technique

Cells were grown to the log phase in YNB medium containing glycerol (SG). The cells were collected, washed, and incubated for 1 h in YNB medium containing different carbon sources. The cells were fixed with 70 % (v/v) ethanol and stained with DAPI. The fluorescence of EGFP and DAPI-stained images were acquired using an IX73 fluorescence microscope equipped with a DP74 camera and cellSens imaging software (Olympus; Tokyo, Japan).

3. Results

3.1. Role of YlSnf1 in growth of Y. lipolytica on medium containing n-alkane and fatty acids

A deletion mutant of *YlSNF1* (Δ*Ylsnf1*) was generated to examine its function of *YlSNF1* on hydrophobic substrate utilization. Deletion of *YlSNF1* was verified using Southern blot analysis (data not shown). Growth analysis was performed on media containing various carbon sources, including glucose, glycerol, *n*-alkanes (*n*-decane, *n*-dodecane, *n*-tetradecane, and *n*-hexadecane), and fatty acids (lauric acid, myristic acid, palmitic acid, and oleic acid) as shown in Fig. 1. The Δ*Ylsnf1* strain was able to grow on glycerol as well as the wild-type strain but showed a slight growth defect on glucose medium. Δ*Ylsnf1* displayed severe growth defects on a medium containing *n*-alkanes (C10–C16) and slight growth impairment on fatty acids (C12–C16, C18:1). The growth of Δ*Ylsnf1* was recovered when *YlSNF1* was expressed under its native promoter in a low copy plasmid pSNF1. Additionally, biomass measurements confirmed a significant growth defect in Δ*Ylsnf1* on *n*-decane-containing medium (Supplementary Fig. 1). These results suggest that *Yl*Snf1 plays an essential role in the utilization of *n*-alkanes and fatty acids with various carbon numbers in *Y. lipolytica*.

3.2. Subcellular localization of YlSnf1

To gain greater insight into the regulatory role of *Yl*Snf1, the subcellular localization was investigated using *Yl*Snf1 tagged with EGFP (*Yl*Snf1-EGFP). In *S. cerevisiae*, it has been reported that the subcellular localization of *Sc*Snf1 was altered in response to different carbon sources [23]. A low-copy number plasmid, pSNF1-EGFP, was constructed to express *Yl*Snf1 fused with EGFP at its C-terminus

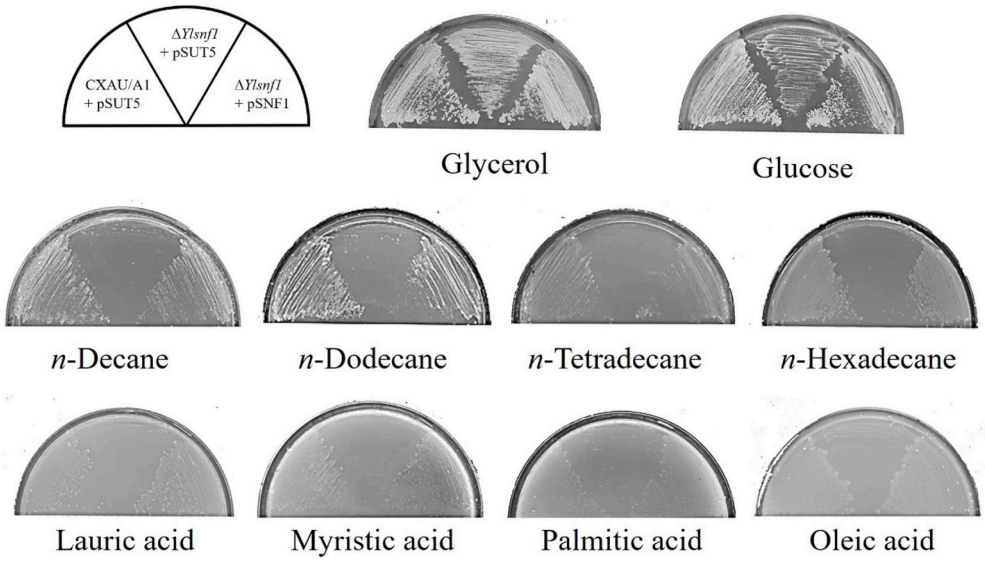

Fig. 1. The growth of the Δ*Ylsnf1* on various carbon sources. Strains were grown at 30 °C for 3 days on glycerol and glucose, or 4 days on oleic acid, palmitic acid myristic acid, lauric acid, *n*-decane, *n*-dodecane, *n*-tetradecane, and *n*-hexadecane. pSUT5 is an empty vector and pSNF1 carries *YlSNF1* under its native promoter.

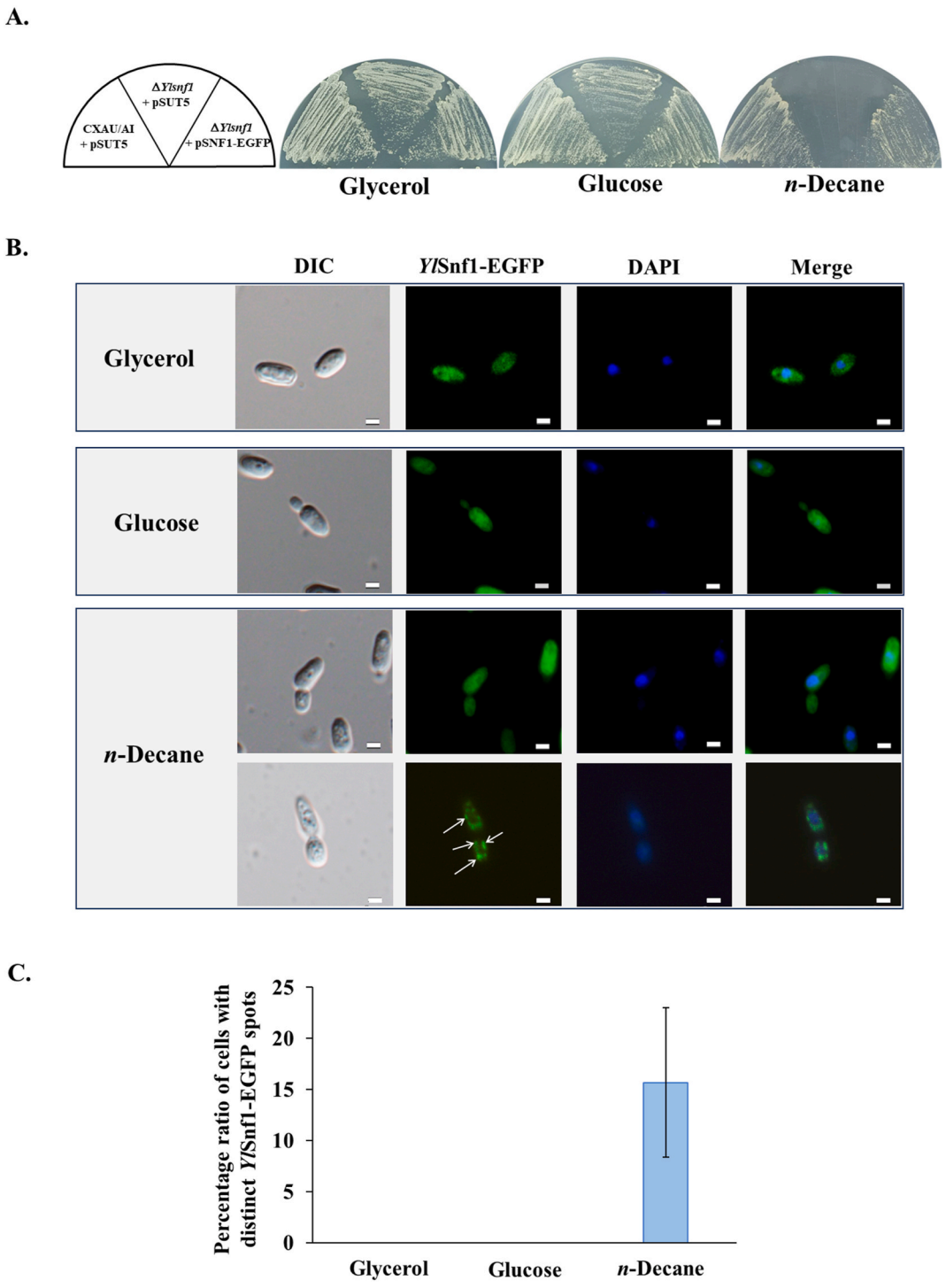

Fig. 2. The subcellular localization of *Yl*Snf1-EGFP. A. The functional analysis of *Yl*Snf1-EGFP was performed by culturing Δ*Ylsnf1* expressing *Yl*Snf1-EGFP on *n*-decane at 30 °C for 4 days. B. The subcellular localization of *Yl*Snf1-EGFP in *Y. lipolytica*. Δ*Ylsnf1* expressing *Yl*Snf1-EGFP was cultivated in SG medium to a logarithmic phase and shifted to glycerol, glucose, or *n*-decane for 1 h. The fluorescence from EGFP and DAPI was observed under an inverted fluorescence microscope (Scale bar represents 2 μm). C. The ratio of the cells with distinct fluorescent spots of *Yl*Snf1-EGFP in the cytosol. Bars indicate the mean and error bars represent the standard deviation of three independent experiments.

from the native promoter of *SNF1*. When this plasmid was introduced into Δ*Ylsnf1*, the growth of Δ*Ylsnf1* was restored to a level similar to that of the wild-type strain on *n*-decane, indicating that *Yl*Snf1-EGFP was functional in *Y. lipolytica* (Fig. 2A). The Δ*Ylsnf1* strain expressing *Yl*Snf1-EGFP was incubated in medium containing glycerol, glucose, or *n*-decane for 1 h, and the fluorescent signals of *Yl*Snf1-EGFP were observed (Fig. 2B). Fluorescent signals of *Yl*Snf1-EGFP were observed in the cytoplasm and nucleus of cells incubated in a medium containing glucose or glycerol. When this strain was incubated in *n*-decane-containing medium, a similar localization pattern of *Yl*Snf1-EGFP was observed, but some cells (approximately 15 %, n = 100) displayed distinct spots of fluorescence signals of *Yl*Snf1-EGFP in the cytosol but not in the nucleus (indicated by white arrows) (Fig. 2B and C). These findings suggest the possibility that *Yl*Snf1 altered its subcellular localization in response to *n*-alkane.

3.3. Role of YlSnf1 in transcription of genes involved in n-alkane utilization

To further elucidate the role of *YlSNF1* on *n*-alkane metabolism in *Y. lipolytica*, transcriptome analysis was performed on the wild-type strain and Δ*Ylsnf1* cultured in a medium containing *n*-decane using RNA-seq. According to the transcriptome data, Δ*Ylsnf1* possessed 433 differentially expressed genes (DEGs) with 302 downregulated and 131 upregulated genes, compared with the wild-type strain, at a 2.5 $\log_2$FC cut-off and adj *P*-value <0.05 (Supplementary Table 1). Among the DEGs, the expression of the *YALI0C00429g* coding for the *Yl*Sip2 β subunit of the Snf1/AMPK complex was substantially downregulated ($\log_2$FC = − 5.2), suggesting a regulatory role of *Yl*Snf1 in the transcription of the *YlSIP2* in *Y. lipolytica* (Table 2). In contrast, no significant change was observed in the expression of the *YALI0E13926g* and *YALI0C03421g* coding for the *Yl*Gal83 β subunit and *Yl*Snf4 γ subunit, respectively (Table 2).

Transcriptome analysis also showed the downregulation of genes associated with various processes of *n*-alkane and fatty acid utilization or their homologs following the deletion of *YlSNF1* (Table 3). The transcript levels of eight *ALK* genes, including *ALK1*, *ALK2*, *ALK3*, *ALK4*, *ALK5*, *ALK6*, *ALK9,* and *ALK11*, whose products have activities to oxidize *n*-alkane or fatty acid except *ALK11*, significantly decreased. Furthermore, the transcript level of *YAS1,* encoding the basic helix-loop-helix transcription factor involved in the transcriptional activation of *ALK1* in response to *n*-alkane, decreased substantially. In addition, Δ*Ylsnf1* exhibited downregulation of 6 alcohol dehydrogenase genes (*ADH1–ADH4*, *ADH6*, and *ADH7*) as well as the fatty alcohol oxidase gene *FAO1* (Supplementary Table 2). A reduction in the transcript levels of the FALDH genes *HFD2* and *HFD3,* involved in the oxidation of fatty aldehydes, was also observed. Furthermore, Δ*Ylsnf1* had substantially diminished expression levels of the 12 acyl-CoA synthetase genes (*FAT1*, *FAT3*, *FAT4*, *AAL1–AAL7*, and *AAL9–AAL10*) and β-oxidation-associated genes (*POX1–6, PAT1, POT1, and MFE2*) [3,7,14]. In addition to genes encoding enzymes involved in *n*-alkane and fatty acid metabolism, the downregulation of genes associated with peroxisome biogenesis was observed in Δ*Ylsnf1*. These results suggested that the transcription of genes involved in the metabolism of *n*-alkane and fatty acid is impaired when *YlSNF1* was deleted. Next, gene ontology (GO) and enriched KEGG pathway analyses were used to explore the roles of the *YlSNF1* in *Y. lipolytica* (Tables 4 and 5, respectively). Both GO and KEGG analyses demonstrated that the genes significantly downregulated in Δ*Ylsnf1* were mainly associated with fatty acid metabolism and peroxisomes. In addition, GO analysis indicated that the transcription of genes associated with CoA-ligase activity, oxidoreductase activity, alcohol dehydrogenase (NAD) activity, heme binding, flavin adenine dinucleotide binding, fatty acid binding, and acyl-CoA oxidase activity, all of which could be involved in the metabolism of *n*-alkane and fatty acids, was significantly diminished in Δ*Ylsnf1*. These results suggest the crucial role of *Yl*Snf1 in the *n*-alkane and fatty acid assimilation of *Y. lipolytica.*

In contrast, the deletion of *YlSnf1* led to a significant upregulation of 131 genes that did not appear to be associated with *n*-alkane or fatty acid metabolism. GO analysis revealed that genes encoding integral components of the plasma membrane were enriched among the upregulated genes. Moreover, enrichment of the KEGG pathway suggested that genes involved in metabolic pathway and biosynthesis of secondary metabolites and amino acids were upregulated in Δ*Ylsnf1*.

To validate the transcriptome analysis, qRT-PCR was used to analyze the transcription of key genes associated with the assimilation of *n*-alkane and fatty acids, including *ALK1–ALK3*, *ALK5*, *ADH7*, *PAT1*, *POT1*, *POX2*, *PEX3*, *PEX11*, *YAS1*, and *HFD3*. In agreement with the RNA-seq analysis, the transcript levels of these genes in Δ*Ylsnf1* greatly decreased compared to those in the wild-type strain (Fig. 3). These results suggest that *Yl*Snf1 is a transcriptional regulator of genes involved in the metabolism of *n*-alkane and fatty acids in *Y. lipolytica*.

3.4. Role of YlSnf1 in utilization of exogenous fatty alcohol and fatty aldehyde

To further clarify the role of *YlSNF1* in the metabolism of hydrophobic substrates, the growth of Δ*Ylsnf1* on fatty alcohol (1-dodecanol) and fatty aldehyde (dodecanal) was analyzed. Δ*Ylsnf1* displayed growth retardation in exogenous 1-dodecanol and dodecanal (Fig. 4). This defect was suppressed by the expression of the gene encoding *Yl*Snf1 tagged with three copies of the HA

Table 2
List of genes involved in a *Yl*Snf1 complex and their transcript levels determined by RNA-seq analysis.

Locus tag	Gene	$\log_2$FC (*snf1/SNF1*)	Adj. P-value	Functions	Ref.
YALI0_C00429g	*SIP2*	−5.20	$8.68E^{-50}$	Sip2: β-subunit of Snf1 protein kinase complex	[26]
YALI0_E13926g	*GAL83*	−0.08	$8.69E^{-1}$	Gal83: β-subunit of Snf1 protein kinase complex	[26]
YALI0_C03421g[a]	*SNF4*	0.47	$2.71E^{-1}$	Snf4: γ-subunit of Snf1 protein kinase complex	[26]

[a] *YALI0_C03421g* was identified as an ortholog of *Sc*Snf4, which encodes a functional protein [26].

Table 3
List of genes involved in the assimilation of *n*-alkane or fatty acid and their homologs, that showed significant changes in the transcript levels in Δ*Ylsnf1*, analyzed by RNA-seq.

Locus tag	Gene	Log_2FC (*snf1*/*SNF1*)	Adj. *P*-value	Functions	Ref.
1. Genes encoding cytochrome P450s in the CYP52-family					
YALI0_B13838g	*ALK5*	−8.17	$2.10E^{-82}$	Alk5: Cytochromes P450: ω-hydroxylation of fatty acid	[10,39,40]
YALI0_B06248g	*ALK9*	−7.23	$2.18E^{-85}$	Alk9: Cytochromes P450: Oxidation of long-carbon chain *n*-alkane (C16–C18)	[10,38,39]
YALI0_C10054g	*ALK11*	−6.72	$1.24E^{-78}$	Alk11: Cytochromes P450: ω-hydroxylation of fatty acid	[10,38,39]
YALI0_E23474g	*ALK3*	−5.03	$4.10E^{-40}$	Alk3: Cytochromes P450: Oxidation of various carbon chain *n*-alkane (C10–C18)	[40]
YALI0_B01848g	*ALK6*	−4.60	$5.18E^{-31}$	Alk6: Cytochromes P450: Oxidation of long-carbon chain *n*-alkane (C16–C18)	[10,38–40]
YALI0_E25982g	*ALK1*	−4.33	$1.26E^{-28}$	Alk1: Cytochromes P450: Oxidation of various carbon chain *n*-alkane (C10–C18) to fatty alcohol	[10,29, 38–40]
YALI0_B13816g	*ALK4*	−3.53	$1.89E^{-25}$	Alk4: Cytochromes P450: ω-hydroxylation of fatty acid	[10,38–40, 50]
YALI0_F01320g	*ALK2*	−3.16	$2.03E^{-13}$	Alk2: Cytochromes P450: Oxidation of long- carbon chain *n*-alkane (C16–C18)	[10,38–40]
2. Genes encoding alcohol dehydrogenases and fatty alcohol oxidase					
YALI0_E07766g	*ADH7*	−8.04	$4.40E^{-68}$	Adh7: Alcohol dehydrogenase 7	[12]
YALI0_D25630g	*ADH1*	−7.36	$1.13E^{-40}$	Adh1: Alcohol dehydrogenase 1: metabolism of exogenous fatty alcohols (C12, C14 & C16)	[12]
YALI0_A16379g	*ADH3*	−6.60	$7.70E^{-54}$	Adh3: Alcohol dehydrogenase 3 metabolism of exogenous fatty alcohols (C12, C14 & C16)	[12]
YALI0_E15818g	*ADH4*	−6.16	$1.54E^{-71}$	Adh4: Alcohol dehydrogenase 4	[12]
YALI0_A15147g	*ADH6*	−4.52	$4.00E^{-32}$	Adh6: Alcohol dehydrogenase 6	[12]
YALI0_E17787g	*ADH2*	−4.44	$2.90E^{-30}$	Adh2: Alcohol dehydrogenase 2	[12]
YALI0_C12595g	*ADH8*	−3.53	$1.30E^{-18}$	Adh8: Alcohol dehydrogenase 8	[51]
3. Genes encoding fatty aldehyde dehydrogenases					
YALI0_A17875g	*HFD3*	−9.52	$2.78E^{-109}$	Hfd3: Fatty aldehyde dehydrogenase 3	[13]
YALI0_E15400g	*HFD2*	−4.62	$1.91E^{-40}$	Hfd2: Fatty aldehyde dehydrogenase 2	[13]
4. Genes encoding acyl-CoA synthetases					
YALI0_F06556g	*AAL5*	−8.87	$6.28E^{-77}$	Aal5: Acyl-CoA synthetase	[52]
YALI0_E05951g	*AAL3*	−7.88	$2.44E^{-89}$	Aal3: Acyl-CoA synthetase	[52]
YALI0_E12419g	*AAL4*	−7.04	$2.87E^{-109}$	Aal4: Acyl-CoA synthetase	[15,52]
YALI0_A14234g	*AAL2*	−6.64	$9.37E^{-35}$	Aal2: Acyl-CoA synthetase	[52]
YALI0_C09284g	*FAT4*	−5.22	$1.49E^{-33}$	Fat4: Acyl-CoA synthetase	[14]
YALI0_B05456g	*FAT3*	−4.71	$7.96E^{-37}$	Fat3: Acyl-CoA synthetase	[14]
YALI0_E16016g	*FAT1*	−4.60	$6.09E^{-31}$	Fat1: Acyl-CoA synthetase	[14]
YALI0_E20405g	*AAL7*	−4.53	$8.29E^{-36}$	Aal7: Acyl-CoA synthetase	[15,52]
YALI0_A15103g	*AAL9*	−4.30	$3.15E^{-24}$	Aal9: Acyl-CoA synthetase	[52]
YALI0_D17314g	*AAL10*	−4.17	$5.29E^{-11}$	Aal10: Acyl-CoA synthetase	[52]
YALI0_C05885g	*AAL6*	−3.76	$3.18E^{-15}$	Aal6: Acyl-CoA synthetase	[52]
YALI0_E11979g	*AAL1*	−2.76	$6.96E^{-09}$	Aal1: Acyl-CoA synthetase	[52]
5. Genes involved in β-oxidation					
YALI0_E27654g	*POX4*	−9.17	$3.90E^{-138}$	Pox4: Peroxisomal acyl-CoA oxidase	[46]
YALI0_E06567g	*POX6*	−8.52	$2.33E^{-131}$	Pox6: Peroxisomal acyl-CoA oxidase	[46]
YALI0_E32835g	*POX1*	−7.80	$7.64E^{-75}$	Pox1: Peroxisomal acyl-CoA oxidase	[46]
YALI0_C23859g	*POX5*	−6.51	$2.32E^{-76}$	Pox5: Peroxisomal acyl-CoA oxidase	[46]
YALI0_E11099g	*PAT1*	−5.69	$4.95E^{-68}$	Pat1: Peroxisomal acetoacetyl-CoA thiolase	[28]
YALI0_D24750g	*POX3*	−5.08	$4.59E^{-56}$	Pox3: Peroxisomal acyl-CoA oxidase	[46]
YALI0_E15378g	*MFE2*	−5.06	$1.25E^{-53}$	Mfe2: Multifunctional enzyme2	[47]
YALI0_F10857g	*POX2*	−4.76	$1.15E^{-44}$	Pox2: Peroxisomal acyl-CoA oxidase	[46]
YALI0_E18568g	*POT1*	−4.02	$4.29E^{-31}$	Pot1: Peroxisomal 3-ketoacyl-thiolase	[48]
6. Genes involved in the transcriptional regulation of *n*-alkane hydroxylation					
YALI0_C02387g	*YAS1*	−4.77	$5.13E^{-33}$	Yas1: Basic Helix-loop-Helix transcription factor: Transcriptional regulation of *ALKs*	[27]
7. Genes involved in peroxisome biogenesis					
YALI0_C04092g	*PEX11*	−4.98	$5.96E^{-41}$	Protein has important role in lipid homeostasis	[53]
YALI0_B19624g	-	−4.09	$8.65E^{-36}$	Unidentified gene: Predicted for Peroxisomal biogenesis factor 3 (Pex3)	[54,55]
YALI0_C18689g	*PEX6*	−3.55	$2.00E^{-30}$	Peroxisomal ATPase, a protein dislocase complex	[56]
YALI0_F01012g	*PEX2*	−3.36	$1.06E^{-25}$	Peroxisome assembly protein PAY5 (Peroxin-2)	[57]
YALI0_C15356g	*PEX1*	−3.23	$1.53E^{-27}$	Peroxisome assembly protein (Peroxin-1)	[56]
YALI0_B22660g	*PEX19*	−3.20	$1.17E^{-22}$	Involvement of peroxisomal membrane proteins (PMP) stability	[58]
YALI0_F22539g	*PEX3*	−3.02	$1.20E^{-17}$	A peroxisomal integral membrane protein required early in peroxisome biogenesis,	[59]
YALI0_F28457g	*PEX5*	−2.92	$6.70E^{-18}$	A Peroxisomal targeting signal 1 (PTS1) receptors	[60]

Table 4
Gene ontology (GO) analysis for DEGs in Δ*Ylsnf1* compared with CXAU/A1 wild-type strain.

GO term	Adj. *P*-value
Downregulation	
Biological process	
Fatty acid beta-oxidation	$2.20E^{-11}$
Secondary metabolic process	$8.20E^{-08}$
Fatty acid beta-oxidation using acyl-CoA oxidase	$2.00E^{-03}$
Cellular component	
Peroxisome	$3.40E^{-14}$
Peroxisomal membrane	$8.60E^{-08}$
Integral component of peroxisomal membrane	$1.20E^{-07}$
Molecular function	
CoA-ligase activity	$7.90E^{-07}$
Enoyl-CoA hydratase activity	$7.90E^{-07}$
Oxidoreductase activity, acting on paired donors, with incorporation or reduction of molecular oxygen, reduced flavin or flavoprotein as one donor, and incorporation of one atom of oxygen	$4.30E^{-05}$
Alcohol dehydrogenase (NAD) activity	$1.10E^{-04}$
Heme binding	$1.30E^{-04}$
Dodecenoyl-CoA delta-isomerase activity	$1.10E^{-03}$
Flavin adenine dinucleotide binding	$1.30E^{-03}$
Fatty acid binding	$2.20E^{-03}$
Acyl-CoA oxidase activity	$2.20E^{-03}$
Iron ion binding	$2.20E^{-03}$
Acyl-CoA hydrolase activity	$2.10E^{-02}$
Upregulation	
Cellular component	
Integral component of plasma membrane	$2.80E^{-03}$
Integral component of membrane	$4.50E^{-02}$
Molecular function	
Copper ion binding	$1.90E^{-03}$

Table 5
KEGG pathway analysis for DEGs in Δ*Ylsnf1* compared with CXAU/A1 wild-type strain.

KEGG Pathway	Adj. *P*-value
Downregulation	
Peroxisome	$5.40E^{-29}$
Fatty acid degradation	$5.50E^{-20}$
Valine, leucine and isoleucine degradation	$3.00E^{-13}$
Carbon metabolism	$6.50E^{-13}$
Metabolic pathways	$3.70E^{-12}$
Biosynthesis of secondary metabolites	$3.70E^{-12}$
Propanoate metabolism	$8.40E^{-10}$
beta-Alanine metabolism	$1.00E^{-09}$
Glyoxylate and dicarboxylate metabolism	$3.20E^{-07}$
Pyruvate metabolism	$3.40E^{-06}$
Fatty acid metabolism	$3.50E^{-06}$
Ubiquinone and other terpenoid-quinone biosynthesis	$6.10E^{-06}$
alpha-Linolenic acid metabolism	$3.30E^{-05}$
Biosynthesis of unsaturated fatty acids	$5.60E^{-05}$
Glycolysis/Gluconeogenesis	$8.80E^{-05}$
Tyrosine metabolism	$2.90E^{-03}$
Tryptophan metabolism	$2.90E^{-03}$
Butanoate metabolism	$8.10E^{-03}$
Pantothenate and CoA biosynthesis	$9.80E^{-03}$
Lysine degradation	$4.80E^{-02}$
Upregulation	
Metabolic pathways	$1.70E^{-05}$
Biosynthesis of secondary metabolites	$1.60E^{-02}$
Biosynthesis of amino acids	$4.90E^{-02}$

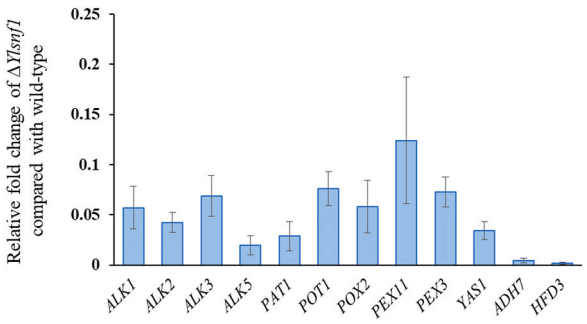

Fig. 3. The relative transcript levels of genes involved in the *n*-alkane and fatty acid utilization. The transcript levels of the genes in Δ*Ylsnf1* and the wild-type strain were analyzed by qRT-PCR. The relative gene expression levels of the genes in Δ*Ylsnf1* to the wild-type strain were determined using a $2^{-\Delta\Delta Cq}$ method. The β-actin gene was used for the normalization.

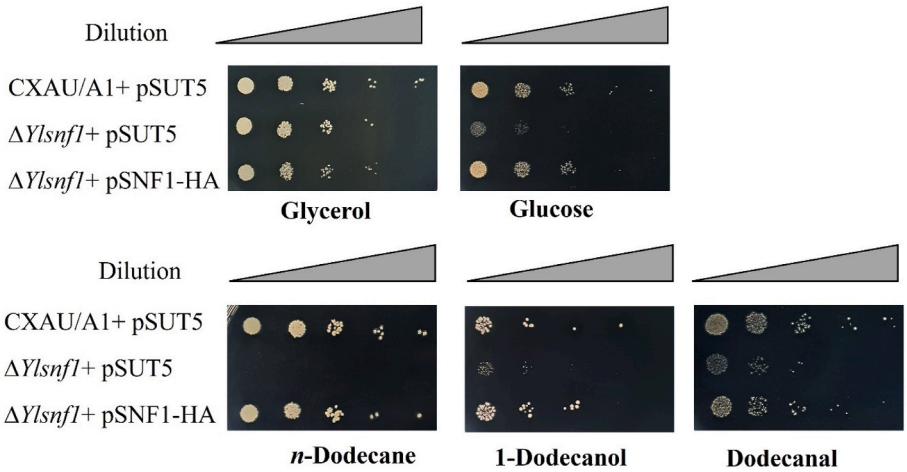

Fig. 4. The growth of Δ*Ylsnf1* on the medium containing fatty alcohol (1-Dodecanol) and fatty aldehyde (Dodecanal). The wild-type strain (CXAU/A1) and Δ*Ylsnf1* containing vector (pSUT5) or the plasmid to express Snf1-HA (pSNF1-HA) were cultured for two days in SG medium and then spotted onto plates with indicated carbon sources in 10-fold serial dilutions. The strains were grown at 30 °C for 2 days on glycerol and glucose or 4 days on *n*-dodecane, 1-dodecanol, and dodecanal.

epitope (*Yl*Snf1-HA), which was shown to be functional because Δ*Ylsnf1* expressing *Yl*Snf1-HA could grow on a medium containing *n*-dodecane. These results suggest the important roles of *Yl*Snf1 in the utilization of intermediates of *n*-alkane metabolism.

4. Discussion

Y. lipolytica is a non-conventional yeast that efficiently uses hydrophobic substrates as its sole carbon source [3,26,30]. In this study, the role of *Yl*Snf1 in the utilization of *n*-alkane in *Y. lipolytica*. Δ*Ylsnf1* showed severe growth defects on *n*-alkane of 10–16 carbons, indicating the vital role of *Yl*Snf1 in the utilization of *n*-alkane of *Y. lipolytica*. Consistent with our findings, the *SNF1/snf1* heterozygote strain of diploid *Candida tropicalis* showed a decrease in cell density compared to the wild-type strain in a medium containing *n*-alkane [31]. In addition, when Δ*snf1* of *Y. lipolytica* was cultured on a glucose-containing medium, slight growth retardation was observed, similar to the deletion mutants of *SNF1* in *S. cerevisiae* and *Candida albicans* [32,33]. The dry cell mass of *Y. lipolytica* with the *YlSNF1* mutation in glucose was not significantly different from that of the wild-type strain, which is in line with a report by Seip et al. [26]. This was potentially due to the high initial inoculum and faster growth kinetics of the cells in the broth culture system [34,35]. In contrast, it has also been reported that Δ*snf1* strain of *Y. lipolytica* expressing three cellulases, ATP citrate lyase, and diacylglycerol acyltransferase genes displayed an increase in cell biomass [26,30]. These differences could probably be due to differences in their genetic backgrounds and the media used.

In *S. cerevisiae*, *Sc*Snf1 is localized in different subcellular compartments, such as the cytoplasm, vacuoles, and nucleus, depending on the growth conditions [23]. The localization of Snf1 is mediated by the β subunit, *Sc*Sip1, *Sc*Sip2, or *ScGal83* [23]. *Sc*Gal83 directs *Sc*Snf1 from the cytoplasm to the nucleus during the shift of the carbon source from glucose to glycerol [23]. In contrast, *Sc*Sip2 was mainly retained in the cytoplasm and responsible for the growth and aging of *S. cerevisiae* [21,33,36,37]. In *Y. lipolytica*, *Yl*Sip2 and *Yl*Gal83 have been identified as orthologs of *Sc*Sip2 and *Sc*Gal83 [26]. *Yl*Snf1 could regulate cellular metabolisms and stress responses

in different cellular compartments by binding to these β subunits. In our findings, the localization pattern of *Yl*Snf1-EGFP as spots in the cytoplasm, excluded from the nucleus in response to *n*-decane, raises the possibility of specific roles of the corresponding β subunit. Transcriptome analysis revealed that the transcript levels of *YlSIP2*, but not *YlGAL83*, substantially decreased in Δ*Ylsnf1*, suggesting a functional relationship between *Yl*Sip2 and *Yl*Snf1 in *Y. lipolytica.* It would be useful to investigate the interaction between the *Yl*Snf1 and its β subunits to portray the association between the function and subcellular localization of the *Yl*Snf1 in response to the *n*-alkane. In addition, it would be of interest to analyze the growth of deletion mutants of *YlSIP2* and *YlGAL83*.

Global transcriptome analysis of Δ*Ylsnf1* revealed numerous downregulated genes involved in *n*-alkane and fatty acid assimilation processes. The transcript levels of eight *ALK* genes, *ALK1*, *ALK2*, *ALK3*, *ALK4*, *ALK5*, *ALK6*, *ALK9* and *ALK11*, which encode CYP52-family P450s, decreased in Δ*Ylsnf1* grown on *n*-decane. Among the Alk proteins, Alk1, Alk2, Alk3, Alk6, Alk9, and Alk10 hydroxylate *n*-alkanes [10]. Moreover, the double deletion mutants of *ALK1* and *ALK2* showed severe growth defects on *n*-alkanes, and the quadruple deletion of *ALK1*, *ALK2*, *ALK4,* and *ALK6* in *Y. lipolytica* resulted in defective growth on *n*-alkane of 10–16 carbons [38]. Although no significant effect was observed on the *ALK10* transcript level by the deletion of *YlSNF1*, the transcript level of *ALK10* was much lower than that of *ALK1*, *ALK2*, *ALK3*, *ALK4*, *ALK6*, or *ALK9* [39]. Therefore, one explanation for the growth defect of Δ*Ylsnf1* in media containing *n*-alkanes could be the reduced transcription levels of these *ALK* genes owing to the deletion of *YlSNF1*. It has been shown that the expression levels of *ALK1* and *ALK2* are highly upregulated in cells incubated in a medium containing *n*-alkanes compared to those in a medium containing glucose in the wild-type strain [39–41]. In this study, the transcript levels of *ALK1* and *ALK2* were greatly downregulated in the deletion mutant of *YlSNF1* cultured in a medium containing *n*-decane. In contrast, Seip et al. reported that the transcript levels of *ALK1* and *ALK2* increased 2.55- and 3.07-folds in a deletion mutant of *YlSNF1* cultured in a medium containing glucose [26]. Therefore, *Yl*Snf1 might be involved not only in the transcriptional repression of *ALK1* and *ALK2* in the absence of *n*-alkane but also in the transcriptional activation of these genes in the presence of *n*-alkane.

Among the eight alcohol dehydrogenase genes, *ADH1–ADH7* and *FADH*, and a fatty alcohol oxidase gene, *FAO1*, the triple deletion mutant of *ADH1, ADH3*, and *FAO1* showed severe growth defects in fatty alcohols [12]. Furthermore, a previous study in *S. cerevisiae* revealed that the transcription of *ADH2* was regulated through Adr1 by *Sc*Snf1 in response to ethanol [42–44]. In our RNA-seq analysis, diminished transcript levels of *ADH* and *FAO1* were also observed by the deletion of *YlSNF1*. Thus, one reason for the growth defects of Δ*Ylsnf1* on exogenous fatty alcohols may be reduced expression of *ADH1*, *ADH3*, and *FAO1*.

In the FALDH genes, the transcript levels of *HFD2* and *HFD3* decreased, whereas significant changes in *HFD1* and *HFD4* were not observed in Δ*Ylsnf1*. Iwama et al. reported that a mutant with a quadruple deletion of *HFD1–HFD4* showed severe growth defects on *n*-alkanes with 12–18 carbons, whereas a double deletion mutant of *HFD2* and *HFD3* grew normally on *n*-alkanes [13]. In addition, the

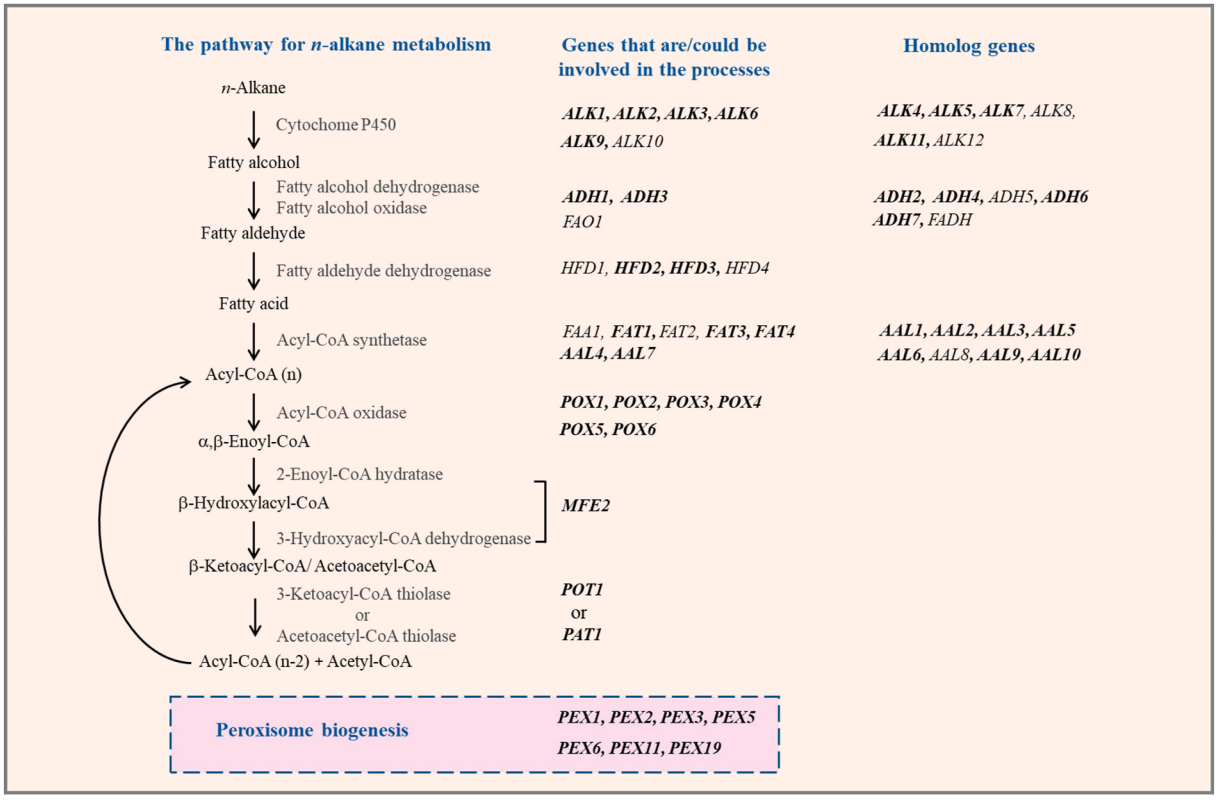

Fig. 5. The metabolic pathway of *n*-alkane with genes involved in the metabolic processes and their regulation in *Y. lipolytica*. The bold gene names denote the DEGs obtained from this study that are downregulated under the control of *Yl*Snf1.

quadruple deletion mutant of *HFD1-HFD4* can grow on a medium containing fatty aldehydes [13]. Therefore, Δ*Ylsnf1* showed growth defects on exogenous fatty aldehydes, probably due to the decreased expression of downstream genes in the metabolic pathway of fatty aldehydes.

In the 15 ACS-coding genes, *FAT1* plays a critical role in the activation of fatty acids produced during the metabolism of *n*-alkanes in the peroxisome for assimilation, while *FAA1* is involved in the activation of fatty acids for lipid synthesis [14,45]. Transcriptomic analysis revealed the downregulation of *FAT1*, but not *FAA1,* in Δ*Ylsnf1*. This suggests that *YlSNF1* is involved in the regulation of the production of fatty-acyl CoAs from fatty acids produced in the metabolism of *n*-alkane for β-oxidation in the peroxisome, not for membrane lipid production in the cytosol [14].

Δ*Ylsnf1* also exhibited defects in the expression of genes involved in β-oxidation. Single deletion mutants of *PAT1*, *POT1*, and *MFE2* and a quadruple deletion mutant of *POX2*, *POX3*, *POX4,* and *POX5* display growth defects in various *n*-alkanes and fatty acids in *Y. lipolytica* [28,46–48]. Furthermore, deletion of *YlSNF1* resulted in the downregulation of various *PEX* genes, including *PEX5*, *PEX6*, and *PEX10*. It was previously shown that the transcription of *ALK1* was decreased by the deletion of *PEX5*, *PEX6*, and *PEX10* [49]. It is possible that the deletion of *YlSNF1* affected the transcription of *ALK* genes by decreasing the expression of these *PEX* genes.

The *ALK* genes are transcriptionally controlled by Yas1, Yas2, and Yas3 [3,16,18,27]. Furthermore, Yas1 induces its expression via autoregulation [27]. Δ*Ylsnf1* exhibited the significant downregulation of *YAS1* regardless of the significant changes in the expression of *YAS2* and *YAS3* in the medium containing *n*-decane. This indicates a regulatory relationship between *YAS1* and *YlSNF1,* in which the expression of *YAS1* is controlled by *Yl*Snf1 and its autoregulation. The transcription of genes involved in fatty acid metabolism, such as *POT1*, is regulated by Por1 [19]. However, the expression of *POR1* was not significantly altered by *n*-decane in Δ*Ylsnf1*, suggesting that *Yl*Snf1 and Por1 may function independently in *Y. lipolytica*.

In conclusion, our findings suggest that *Yl*Snf1 is a crucial regulator for the metabolism of the *n*-alkane in *Y. lipolytica.* The deletion of *YlSNF1* caused growth defects in the medium containing *n*-alkanes, most likely because of the decrease in the expression of genes involved in *n*-alkane metabolism (Fig. 5). The insights obtained in this study will contribute to the advanced application of *Y. lipolytica* in the bioconversion of *n*-alkane to various chemicals and the bioremediation of petroleum-contaminated environments. However, the mechanism through which *Yl*Snf1 regulates the transcription of genes involved in *n*-alkane assimilation remains unclear. Further investigation into the molecular mechanism of *Yl*Snf1 in the regulation of *n*-alkane metabolism could pave the way for a deeper understanding of the response to *n*-alkane in *Y. lipolytica*.

Funding

This work was supported by NSRF via the Program Management Unit for Human Resources & Institutional Development, Research and Innovation (grant number B05F640109) to PK and Kasetsart University Research and Development Institute (grant numbers P–Y (D)19.60, P-3.2(D)21.60) to NP, and International SciKU Branding (ISB), Faculty of Science, Kasetsart University, Thailand.

Data availability statement

The raw FASTQ data associated with this study has been deposited in the GEO database (GSE 215766) and available upon request.

CRediT authorship contribution statement

Napapol Poopanitpan: Writing – review & editing, Writing – original draft, Visualization, Supervision, Methodology, Investigation, Funding acquisition, Formal analysis, Data curation, Conceptualization. **Sorawit Piampratom:** Visualization, Investigation, Data curation. **Patthanant Viriyathanit:** Visualization, Investigation. **Threesara Lertvatasilp:** Investigation. **Hiroyuki Horiuchi:** Writing – review & editing, Resources. **Ryouichi Fukuda:** Writing – review & editing, Resources. **Pichamon Kiatwuthinon:** Writing – review & editing, Writing – original draft, Visualization, Supervision, Methodology, Funding acquisition, Formal analysis, Data curation, Conceptualization.

Declaration of competing interest

The authors declare that they have no known competing financial interests or personal relationships that could have appeared to influence the work reported in this paper.

Acknowledgements

The authors would like to acknowledge Department of Biochemistry, Faculty of Science, Kasetsart University for laboratory equipment.

Abbreviations

Acyl-CoA synthetase, ACS
AMP-activated protein kinase, AMPK
Alkane-responsive element 1, ARE1

Basic helix-loop-helix, bHLH
4′,6-diamidino-2-phenylindole, DAPI
Differential interference contrast, DIC
Differentially expressed genes, DEGs
Endoplasmic reticulum, ER
Enhanced green fluorescent protein, EGFP
Fatty alcohol dehydrogenase, FADH
Fatty alcohol oxidase, FAO
Fatty aldehyde dehydrogenases, FADLH
RNA sequencing, RNA-seq
Sucrose non-fermenting 1, Snf1
Yeast nitrogen base, YNB

Appendix A. Supplementary data

Supplementary data to this article can be found online at https://doi.org/10.1016/j.heliyon.2024.e32886.

References

[1] G. Barth, C. Gaillardin, Physiology and genetics of the dimorphic fungus *Yarrowia lipolytica*, FEMS Microbiol. Rev. 19 (1997) 219–237, https://doi.org/10.1111/j.1574-6976.1997.tb00299.x.

[2] S.-Y. Zeng, H.-H. Liu, T.-Q. Shi, P. Song, L.-J. Ren, H. Huang, X.-J. Ji, Recent advances in metabolic engineering of *Yarrowia lipolytica* for lipid overproduction, Eur. J. Lipid Sci. Technol. 120 (2018) 1700352, https://doi.org/10.1002/ejlt.201700352.

[3] R. Fukuda, Metabolism of hydrophobic carbon sources and regulation of it in *n*-alkane-assimilating yeast *Yarrowia lipolytica*, Biosci. Biotechnol. Biochem. 77 (2013) 1149–1154, https://doi.org/10.1271/bbb.130164.

[4] O.E. Csutak, N.-O. Nicula, E.-M. Lungulescu, V. Marinescu, V.M.J.A.S. Corbu, *Yarrowia lipolytica* CMGB32 biosurfactants produced using *n*-hexadecane: developing strategies for environmental remediation, Appl. Sci. 14 (2024) 3048, https://doi.org/10.3390/app14073048.

[5] M. Lopes, S.M. Miranda, A.R. Costa, A.S. Pereira, I. Belo, *Yarrowia lipolytica* as a biorefinery platform for effluents and solid wastes valorization – challenges and opportunities, Crit. Rev. Biotechnol. 42 (2022) 163–183, https://doi.org/10.1080/07388551.2021.1931016.

[6] R. Fukuda, Utilization of *n*-alkane and roles of lipid transfer proteins in *Yarrowia lipolytica*, World J. Microbiol. Biotechnol. 39 (2023) 97, https://doi.org/10.1007/s11274-023-03541-3.

[7] P. Fickers, P.H. Benetti, Y. Waché, A. Marty, S. Mauersberger, M.S. Smit, J.M. Nicaud, Hydrophobic substrate utilisation by the yeast *Yarrowia lipolytica*, and its potential applications, FEMS Yeast Res. 5 (2005) 527–543, https://doi.org/10.1016/j.femsyr.2004.09.004.

[8] R. Fukuda, A. Ohta, Utilization of hydrophobic substrate by *Yarrowia lipolytica*, in: G. Barth (Ed.), Yarrowia Lipolytica: Genetics, Genomics, and Physiology, Springer Berlin Heidelberg, Berlin, Heidelberg, 2013, pp. 111–119, https://doi.org/10.1007/978-3-642-38320-5_5.

[9] R. Fukuda, A. Ohta, Enzymes for aerobic degradation of alkanes in yeasts, in: F. Rojo (Ed.), Aerobic Utilization of Hydrocarbons, Oils and Lipids, Springer International Publishing, Cham, 2017, pp. 1–14, https://doi.org/10.1007/978-3-319-39782-5_7-1.

[10] R. Iwama, S. Kobayashi, C. Ishimaru, A. Ohta, H. Horiuchi, R. Fukuda, Functional roles and substrate specificities of twelve cytochromes P450 belonging to CYP52 family in *n*-alkane assimilating yeast *Yarrowia lipolytica*, Fungal Genet. Biol. 91 (2016) 43–54, https://doi.org/10.1016/j.fgb.2016.03.007.

[11] K. Mori, R. Iwama, S. Kobayashi, H. Horiuchi, R. Fukuda, A. Ohta, Transcriptional repression by glycerol of genes involved in the assimilation of *n*-alkanes and fatty acids in yeast *Yarrowia lipolytica*, FEMS Yeast Res. 13 (2013) 233–240, https://doi.org/10.1111/1567-1364.12025.

[12] R. Iwama, S. Kobayashi, A. Ohta, H. Horiuchi, R. Fukuda, Alcohol dehydrogenases and an alcohol oxidase involved in the assimilation of exogenous fatty alcohols in *Yarrowia lipolytica*, FEMS Yeast Res. 15 (2015), https://doi.org/10.1093/femsyr/fov014.

[13] R. Iwama, S. Kobayashi, A. Ohta, H. Horiuchi, R. Fukuda, Fatty aldehyde dehydrogenase multigene family involved in the assimilation of *n*-alkanes in *Yarrowia lipolytica*, J. Biol. Chem. 289 (2014) 33275–33286, https://doi.org/10.1074/jbc.M114.596890.

[14] Tenagy, J.S. Park, R. Iwama, S. Kobayashi, A. Ohta, H. Horiuchi, R. Fukuda, Involvement of acyl-CoA synthetase genes in n-alkane assimilation and fatty acid utilization in yeast *Yarrowia lipolytica*, FEMS Yeast Res. 15 (2015) fov031, https://doi.org/10.1093/femsyr/fov031.

[15] R. Iwama Tenagy, S. Kobayashi, Y. Shiwa, H. Yoshikawa, H. Horiuchi, R. Fukuda, S. Kajiwara, Acyl-CoA synthetases, Aal4 and Aal7, are involved in the utilization of exogenous fatty acids in *Yarrowia lipolytica*, J. Gen. Appl. Microbiol. 67 (2021) 9–14, https://doi.org/10.2323/jgam.2020.03.001.

[16] S. Kobayashi, K. Hirakawa, H. Horiuchi, R. Fukuda, A. Ohta, Phosphatidic acid and phosphoinositides facilitate liposome association of Yas3p and potentiate derepression of ARE1 (alkane-responsive element one)-mediated transcription control, Fungal Genet. Biol. 61 (2013) 100–110, https://doi.org/10.1016/j.fgb.2013.09.008.

[17] R. Fukuda, A. Ohta, Genetic features and regulation of *n*-alkane metabolism in yeasts, in: F. Rojo (Ed.), Aerobic Utilization of Hydrocarbons, Oils and Lipids, Springer International Publishing, Cham, 2017, pp. 1–13, https://doi.org/10.1007/978-3-319-39782-5_24-1.

[18] S. Endoh-Yamagami, K. Hirakawa, D. Morioka, R. Fukuda, A. Ohta, Basic helix-loop-helix transcription factor heterocomplex of Yas1p and Yas2p regulates cytochrome P450 expression in response to alkanes in the yeast *Yarrowia lipolytica*, Eukaryot. Cell 6 (2007) 734–743, https://doi.org/10.1128/EC.00412-06.

[19] N. Poopanitpan, S. Kobayashi, R. Fukuda, H. Horiuchi, A. Ohta, An ortholog of *farA* of *Aspergillus nidulans* is implicated in the transcriptional activation of genes involved in fatty acid utilization in the yeast *Yarrowia lipolytica*, Biochem. Biophys. Res. Commun. 402 (2010) 731–735, https://doi.org/10.1016/j.bbrc.2010.10.096.

[20] P. Sanz, R. Viana, M.A. Garcia-Gimeno, AMPK in yeast: the SNF1 (sucrose non-fermenting 1) protein kinase complex, in: M.D. Cordero, B. Viollet (Eds.), AMP-Activated Protein Kinase, Springer International Publishing, Cham, 2016, pp. 353–374, https://doi.org/10.1007/978-3-319-43589-3_14.

[21] K. Ashrafi, S.S. Lin, J.K. Manchester, J.I. Gordon, Sip2p and its partner snf1p kinase affect aging in *S. cerevisiae*, Genes Dev. 14 (2000) 1872–1885, https://doi.org/10.1101/gad.14.15.1872.

[22] S. Zaman, S.I. Lippman, X. Zhao, J.R. Broach, How Saccharomyces responds to nutrients, Annu. Rev. Genet. 42 (2008) 27–81, https://doi.org/10.1146/annurev.genet.41.110306.130206.

[23] O. Vincent, R. Townley, S. Kuchin, M. Carlson, Subcellular localization of the Snf1 kinase is regulated by specific beta subunits and a novel glucose signaling mechanism, Genes Dev. 15 (2001) 1104–1114, https://doi.org/10.1101/gad.879301.

[24] K. Hedbacker, M. Carlson, Regulation of the nucleocytoplasmic distribution of snf1-gal83 protein kinase, Eukaryot. Cell 5 (2006) 1950, https://doi.org/10.1128/EC.00256-06.

[25] L. Meng, H.-L. Liu, X. Lin, X.-P. Hu, K.-R. Teng, S.-X. Liu, Enhanced multi-stress tolerance and glucose utilization of *Saccharomyces cerevisiae* by overexpression of the *SNF1* gene and varied beta isoform of Snf1 dominates in stresses, Microb. Cell Factories 19 (2020) 134, https://doi.org/10.1186/s12934-020-01391-4.

[26] J. Seip, R. Jackson, H. He, Q. Zhu, S.-P. Hong, Snf1 is a regulator of lipid accumulation in *Yarrowia lipolytica*, Appl. Environ. Microbiol. 79 (2013) 7360–7370, https://doi.org/10.1128/AEM.02079-13.

[27] S. Yamagami, D. Morioka, R. Fukuda, A. Ohta, A basic helix-loop-helix transcription factor essential for cytochrome p450 induction in response to alkanes in yeast *Yarrowia lipolytica*, J. Biol. Chem. 279 (2004) 22183–22189, https://doi.org/10.1074/jbc.M313313200.

[28] S. Yamagami, T. Iida, Y. Nagata, A. Ohta, M. Takagi, Isolation and characterization of acetoacetyl-CoA thiolase gene essential for *n*-decane assimilation in yeast *Yarrowia lipolytica*, Biochem. Biophys. Res. Commun. 282 (2001) 832–838, https://doi.org/10.1006/bbrc.2001.4653.

[29] T. Iida, A. Ohta, M. Takagi, Cloning and characterization of an *n*-alkane-inducible cytochrome P450 gene essential for *n*-decane assimilation by *Yarrowia lipolytica*, Yeast 14 (1998) 1387–1397, https://doi.org/10.1002/(SICI)1097-0061(199811)14:15<1387::AID-YEA333>3.0.CO;2-M.

[30] H. Wei, W. Wang, E.P. Knoshaug, X. Chen, S. Van Wychen, Y.J. Bomble, M.E. Himmel, M. Zhang, Disruption of the Snf1 gene enhances cell growth and reduces the metabolic burden in cellulase-expressing and lipid-accumulating *Yarrowia lipolytica*, Front. Microbiol. 12 (2021), https://doi.org/10.3389/fmicb.2021.757741.

[31] T. Kanai, K. Ogawa, M. Ueda, A.J.A.o.m. Tanaka, Expression of the SNF1 gene from *Candida tropicalis* is required for growth on various carbon sources, including glucose, Arch. Microbiol. 172 (1999) 256–263, https://doi.org/10.1007/s002030050768.

[32] A. Mottola, S. Schwanfelder, J. Morschhäuser, Generation of viable *Candida albicans* mutants lacking the "essential" protein kinase Snf1 by inducible gene deletion, mSphere 5 (2020), https://doi.org/10.1128/mSphere.00805-20.

[33] M.C. Schmidt, R.R. McCartney, β-subunits of Snf1 kinase are required for kinase function and substrate definition, EMBO J. 19 (2000) 4936–4943, https://doi.org/10.1093/emboj/19.18.4936.

[34] E.M. Rivas, E. Gil de Prado, P. Wrent, M.I. de Silóniz, P. Barreiro, E.C. Correa, F. Conejero, A. Murciano, J.M. Peinado, A simple mathematical model that describes the growth of the area and the number of total and viable cells in yeast colonies, Lett. Appl. Microbiol. 59 (2014) 594–603, https://doi.org/10.1111/lam.12314.

[35] J.R. Meunier, M. Choder, Saccharomyces cerevisiae colony growth and ageing: biphasic growth accompanied by changes in gene expression, Yeast 15 (1999) 1159–1169, https://doi.org/10.1002/(sici)1097-0061(19990915)15:12<1159::Aid-yea441>3.0.Co;2-d.

[36] S.S. Lin, J.K. Manchester, J.I. Gordon, Sip2, an N-Myristoylated β subunit of Snf1 kinase, regulates aging in *Saccharomyces cerevisiae* by affecting cellular histone kinase activity, recombination at rDNA loci, and silencing, J. Biol. Chem. 278 (2003) 13390–13397, https://doi.org/10.1074/jbc.M212818200.

[37] R. Jiao, S. Postnikoff, T.A. Harkness, T.G. Arnason, The *SNF1* kinase ubiquitin-associated domain restrains its activation, activity, and the yeast life span, J. Biol. Chem. 290 (2015) 15393–15404, https://doi.org/10.1074/jbc.M115.647032.

[38] H. Takai, R. Iwama, S. Kobayashi, H. Horiuchi, R. Fukuda, A. Ohta, Construction and characterization of a *Yarrowia lipolytica* mutant lacking genes encoding cytochromes P450 subfamily 52, Fungal Genet. Biol. 49 (2012) 58–64, https://doi.org/10.1016/j.fgb.2011.11.003.

[39] K. Hirakawa, S. Kobayashi, T. Inoue, S. Endoh-Yamagami, R. Fukuda, A. Ohta, Yas3p, an Opi1 family transcription factor, regulates cytochrome P450 expression in response to n-alkanes in *Yarrowia lipolytica*, J. Biol. Chem. 284 (2009) 7126–7137, https://doi.org/10.1074/jbc.M806864200.

[40] T. Lida, T. Sumita, A. Ohta, M. Takagi, The cytochrome P450ALK multigene family of an n-alkane-assimilating yeast, *Yarrowia lipolytica*: cloning and characterization of genes coding for new CYP52 family members, Yeast 16 (2000) 1077–1087, https://doi.org/10.1002/1097-0061(20000915)16:12.

[41] N. Watanabe, R. Iwama, R. Murayama, T. Suzawa, Z. He, A. Mizuike, Y. Shiwa, H. Yoshikawa, H. Horiuchi, R. Fukuda, Orthologs of *Saccharomyces cerevisiae* SFH2, genes encoding Sec14 family proteins, implicated in utilization of *n*-alkanes and filamentous growth in response to *n*-alkanes in *Yarrowia lipolytica*, FEMS Yeast Res. 22 (2022), https://doi.org/10.1093/femsyr/foac006.

[42] O. de Smidt, J.C. du Preez, J. Albertyn, The alcohol dehydrogenases of *Saccharomyces cerevisiae*: a comprehensive review, FEMS Yeast Res. 8 (2008) 967–978, https://doi.org/10.1111/j.1567-1364.2008.00387.x.

[43] O. de Smidt, J.C. du Preez, J. Albertyn, Molecular and physiological aspects of alcohol dehydrogenases in the ethanol metabolism of *Saccharomyces cerevisiae*, FEMS Yeast Res. 12 (2012) 33–47, https://doi.org/10.1111/j.1567-1364.2011.00760.x.

[44] E.T. Young, N. Kacherovsky, K. Van Riper, Snf1 protein kinase regulates Adr1 binding to chromatin but not transcription activation, J. Biol. Chem. 277 (2002) 38095–38103, https://doi.org/10.1074/jbc.M206158200.

[45] R. Dulermo, H. Gamboa-Melendez, T. Dulermo, F. Thevenieau, J.M. Nicaud, The fatty acid transport protein Fat1p is involved in the export of fatty acids from lipid bodies in *Yarrowia lipolytica*, FEMS Yeast Res. 14 (2014) 883–896, https://doi.org/10.1111/1567-1364.12177.

[46] H. Wang, M.T. Le Dall, Y. Wache, C. Laroche, J.M. Belin, J.M. Nicaud, Cloning, sequencing, and characterization of five genes coding for acyl-CoA oxidase isozymes in the yeast *Yarrowia lipolytica*, Cell Biochem. Biophys. 31 (1999) 165–174, https://doi.org/10.1007/BF02738170.

[47] J.J. Smith, T.W. Brown, G.A. Eitzen, R.A. Rachubinski, Regulation of peroxisome size and number by fatty acid-oxidation in the yeast *Yarrowia lipolytica*, J. Biol. Chem. 275 (2000) 20168–20178, https://doi.org/10.1074/jbc.M909285199.

[48] G. Berninger, R. Schmidtchen, G. Casel, A. Knorr, K. Rautenstrauss, W.H. Kunau, E. Schweizer, Structure and metabolic control of the *Yarrowia lipolytica* peroxisomal 3-oxoacyl-CoA-thiolase gene, Eur. J. Biochem. 216 (1993) 607–613, https://doi.org/10.1111/j.1432-1033.1993.tb18180.x.

[49] T. Sumita, T. Iida, A. Hirata, H. Horiuchi, M. Takagi, A. Ohta, Peroxisome deficiency represses the expression of n-alkane-inducible *YlALK1* encoding cytochrome P450ALK1 in *Yarrowia lipolytica*, FEMS Microbiol. Lett. 214 (2002) 31–38, https://doi.org/10.1111/j.1574-6968.2002.tb11321.x.

[50] T. Sumita, T. Iida, S. Yamagami, H. Horiuchi, M. Takagi, A. Ohta, *YlALK1* encoding the cytochrome P450ALK1 in *Yarrowia lipolytica* is transcriptionally induced by *n*-alkane through two distinct cis-elements on its promoter, Biochem. Biophys. Res. Commun. 294 (2002) 1071–1078, https://doi.org/10.1016/S0006-291X(02)00607-1.

[51] M. Gatter, A. Förster, K. Bär, M. Winter, C. Otto, P. Petzsch, M. Ježková, K. Bahr, M. Pfeiffer, F. Matthäus, G. Barth, A newly identified fatty alcohol oxidase gene is mainly responsible for the oxidation of long-chain ω-hydroxy fatty acids in *Yarrowia lipolytica*, FEMS Yeast Res. 14 (2014) 858–872, https://doi.org/10.1111/1567-1364.12176.

[52] R. Dulermo, H. Gamboa-Melendez, R. Ledesma-Amaro, F. Thevenieau, J.M. Nicaud, *Yarrowia lipolytica AAL* genes are involved in peroxisomal fatty acid activation, Biochim. Biophys. Acta, Mol. Cell Biol. Lipids 1861 (2016) 555–565, https://doi.org/10.1016/j.bbalip.2016.04.002.

[53] R. Dulermo, T. Dulermo, H. Gamboa-Meléndez, F. Thevenieau, J.-M. Nicaud, Role of Pex11p in lipid homeostasis in *Yarrowia lipolytica*, Eukaryot. Cell 14 (2015) 511–525, https://doi.org/10.1128/ec.00051-15.

[54] A. Schlüter, A. Real-Chicharro, T. Gabaldón, F. Sánchez-Jiménez, A. Pujol, PeroxisomeDB 2.0: an integrative view of the global peroxisomal metabolome, Nucleic Acids Res. 38 (2009) D800–D805, https://doi.org/10.1093/nar/gkp935.

[55] T.U. Consortium, UniProt: the universal protein knowledgebase in 2023, Nucleic Acids Res. 51 (2023) D523–d531, https://doi.org/10.1093/nar/gkac1052.

[56] V.I. Titorenko, J.J. Smith, R.K. Szilard, R.A. Rachubinski, Peroxisome biogenesis in the yeast *Yarrowia lipolytica*, Cell Biochem. Biophys. 32 (2000) 21–26, https://doi.org/10.1385/CBB:32:1-3:21.

[57] G.A. Eitzen, V.I. Titorenko, J.J. Smith, M. Veenhuis, R.K. Szilard, R.A. Rachubinski, The *Yarrowia lipolytica* gene *PAY5* encodes a peroxisomal integral membrane protein homologous to the mammalian peroxisome assembly factor PAF-1, J. Biol. Chem. 271 (1996) 20300–20306, 0.1074/jbc.271.34.20300.

[58] G.R. Lambkin, R.A. Rachubinski, *Yarrowia lipolytica* cells mutant for the peroxisomal peroxin Pex19p contain structures resembling wild-type peroxisomes, Mol. Biol. Cell 12 (2001) 3353–3364, https://doi.org/10.1091/mbc.12.11.3353.

[59] R.A. Bascom, H. Chan, R.A. Rachubinski, Peroxisome biogenesis occurs in an unsynchronized manner in close association with the endoplasmic reticulum in temperature-sensitive *Yarrowia lipolytica* Pex3p mutants, Mol. Biol. Cell 14 (2002) 939–957, https://doi.org/10.1091/mbc.e02-10-0633.

[60] R.K. Szilard, R.A. Rachubinski, Tetratricopeptide repeat domain of *Yarrowia lipolytica* Pex5p is essential for recognition of the type 1 peroxisomal targeting signal but does not confer full biological activity on Pex5p, Biochem. J. 346 (1) (2000) 177–184, https://doi.org/10.1042/bj3460177.